SAND2015-4299C

Dependence on Geographic Location of Air Mass Modifiers For Photovoltaic Module Performance Models

Katherine A. Klise, Clifford W. Hansen, Joshua S. Stein

Sandia National Laboratories, Albuquerque, NM 87185, USA

***Abstract* — Air mass modifiers are frequently used to represent the effects of solar spectrum on PV module current. Existing PV module performance models assume a single empirical expression, a polynomial in air mass, for all locations and times. In this paper, air mass modifiers are estimated for several modules of different types from IV curves measured with the modules at fixed orientation in three climatically different locations around the United States. Systematic variation is found in the effect of solar spectrum on PV module current that is not well approximated by the standard air mass modifier polynomial.**

***Index Terms* — air mass modifier, monitored system data, photovoltaic, solar spectrum, system performance.**

I. Introduction

Variations in the solar spectrum from optical air mass and from atmospheric conditions can cause changes in a module's short circuit current. These effects are most frequently represented in module performance models (e.g., the Sandia Photovoltaic Array Performance Model (SAPM) [1] and the De Soto single diode model [2]) by a multiplier on module current formulated as an empirical polynomial in absolute air mass, AM_a. The air mass function, $f_1(AM_a)$, is typically determined by module testing outdoors under cloudless skies [3], [4]. Coefficients for the empirical function have been reported for many modules with different cell types [5]. Conventional practice views the air mass function as an invariant description of a module's behavior in any climate.

As has been noted by other authors [6], use of the fixed air mass function entails several assumptions about the function itself. For example, paraphrasing from [6], changes in module current normalized for broadband irradiance and cell temperature are assumed to be a function only of air mass, which itself is determined by solar elevation angle and atmospheric pressure. However, it is reasonable to expect that the solar spectral content can vary apart from broadband irradiance and air mass; for example, due to water vapor content or atmospheric turbidity. Outdoor testing at Sandia National Laboratories (Sandia) provides evidence of the effect of this variation on normalized module current with I_{SC} frequently lower in the afternoon than in the morning at the same air mass [7]. Consequently it is reasonable to accept the hypothesis that the air mass function may depend on location and climate as well as on a PV module's cells.

To our knowledge there are few, if any, investigations into the potential variability of a module's air mass function across locations with varying climate. Osterwald et al. [6] published an analysis demonstrating that the air mass modifier can vary over time at a fixed location. Andrews et al. [8] analyzed an air mass modifier very similar to the SAPM formulation using data obtained from modules on fixed tilt racking at a single location in Canada. They note that their results differ systematically from the air mass modifiers published by Sandia for modules of similar type.

The variation in air mass functions at different locations has not previously been explored because suitable data and appropriate analysis techniques have not been available. Ideally, the data would comprise measurements of the same modules outdoors at a variety of locations. Recently the National Renewable Energy Laboratory (NREL) has made available measured output from the mobile Performance and Energy Rating Testbed (mPERT) which includes a set of modules deployed at three climatically different locations around the United States: Cocoa, Florida (subtropical climate), Eugene, Oregon (marine west coast climate), and Golden, Colorado (semi-arid climate) [9]. Sandia has recently developed and tested a method to determine air mass modifiers, and other model parameters, from IV curves measured for modules at fixed tilt orientation [7], [10]. Portions of the Sandia method are similar to the approach published in [8] which addresses extracting parameters for prediction of I_{SC} from data obtained from fixed tilt racking.

In this paper, we describe our methods to estimate the air mass modifier polynomial, $f_1(AM_a)$, and associated short-circuit current at standard test conditions (STC), I_{SC0}, using data collected outdoors for modules on fixed racking. The method is then used to investigate systematic dependence of $f_1(AM_a)$ and I_{SC0} on time of year and location using mPERT data.

II. mPERT Data

The mPERT dataset includes IV curves and meteorological data for PV modules set at fixed tilt orientation at three locations that differ in their climatic conditions. The dataset includes eleven modules covering a range of cell technologies. The same modules deployed at Cocoa were later deployed at Eugene. At both locations, data was collected every five minutes for approximately a year. A second set of the modules of the same model and manufacturer were deployed in Golden, where data was collected every fifteen minutes for approximately a year. The datasheet specifications for modules used at Cocoa and Eugene differ slightly from datasheet specifications for modules used at Golden.

Although GHI, DHI, and DNI measurements are available, we chose to use only plane of array irradiance, G_{POA}, measured using a CMP 22 pyranometer, for model calibration in order that our methods could be broadly applicable. I_{SC}, I_{MP}, V_{OC}, V_{MP}, and P_{MP} are extracted from each IV curve. Module back-surface temperature was converted to cell temperature using methods described in [1]. AM_a and AOI are computed using the module's orientation and solar ephemerides.

Absolute humidity is computed for each site to explore how the air mass modifier might be influenced by water vapor content. Absolute humidity is a function of the relative humidity, pressure, and ambient air temperature based on methods described in [11] (Fig. 1). At all three sites, absolute humidity approximately doubles in the summer.

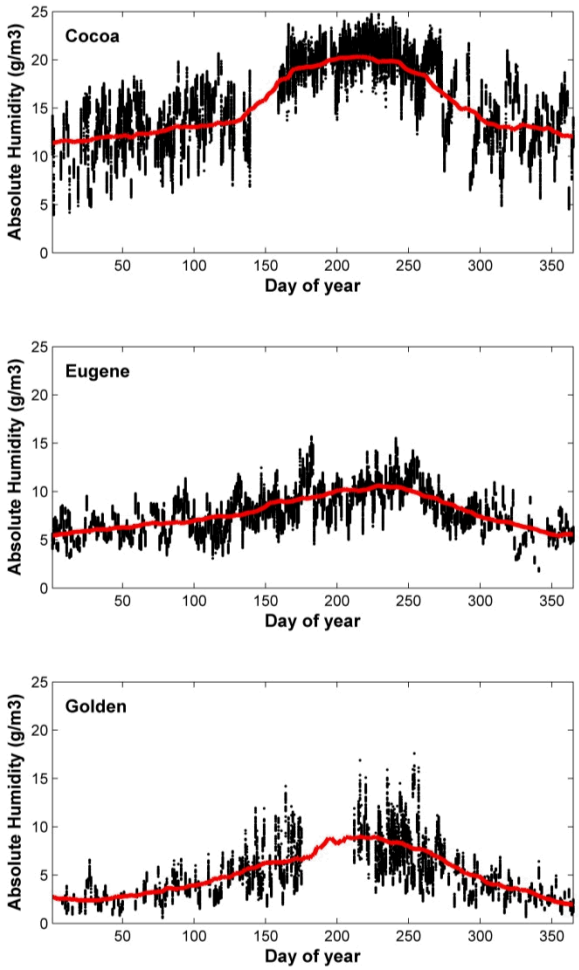

Fig. 1. Absolute humidity (black dots) at mPERT locations along with the 30 day moving average at solar noon (red line).

Before using the mPERT data to estimate $f_1(AM_a)$ and I_{SC0}, several filters are applied to eliminate erroneous or inconsistent data. These filters include (1) removing data with physically unreasonable values, (2) removing data with high AM_a (> 6.5) or AOI (> 70) because irradiance measurements at these conditions are generally less reliable, and (3) removing data when the G_{POA} and I_{SC} are not linearly correlated.

III. Methods

Methods to calibrate the SAPM using data from modules on fixed tilt racking are outlined in [7], [10]. Techniques to estimate $f_1(AM_a)$ and I_{SC0} are explained in detail here.

In the SAPM, short-circuit current I_{SC} is calculated as

$$I_{SC} = I_{SC0} f_1(AM_a) \frac{E}{E_0}\left(1+\alpha_{SC}\left(T_C - T_0\right)\right) \quad (1)$$

where I_{SC0} is the short-circuit current at STC, $f_1(AM_a)$ is the air mass modifier, E is the broadband plane of array irradiance that reaches the module's cells, E_0 is the reference irradiance set to 1000 W/m^2, and the factor $1+\alpha_{SC}\left(T_C - T_0\right)$ adjusts I_{SC} for cell temperature T_C. A very similar air mass modifier is used in the De Soto single diode model [2]. The broadband irradiance that reaches a module's cells is calculated as

$$E = E_b f_2(AOI) + f_d E_{diff} \quad (2)$$

where E_b and E_{diff} are respectively beam and diffuse broadband irradiance (W/m^2) on the module's face. In this analysis, the fraction of beam irradiance that is not reflected from the module's face, $f_2(AOI)$, was defined by [10] using an angular loss coefficient of 0.13, and the fraction of diffuse irradiance used by module, f_d, was set to 1.

Using Eq. 1 and 2, I_{SC0} and $f_1(AM_a)$ are estimated during clear-sky conditions. For I_{SC0}, observations are selected where $1 \le AM_a \le 2$ and $E \approx 1000$ W/m^2, irradiance and temperature adjusted I_{SC} is fit as a polynomial in AM_a by regression:

$$\frac{I_{SC}}{1+\alpha_{SC}\left(T_C - T_0\right)}\frac{E_0}{E} = \beta_0 + \beta_1 AM_a + \beta_2 AM_a^2 \quad (3)$$

and I_{SC0} is set to the polynomial's value at $AM_a = 1.5$

$$I_{SC0} = \beta_0 + 1.5\beta_1 + 2.25\beta_2 \quad (4)$$

With I_{SC0} in hand, $f_1(AM_a)$ is estimated by fitting a polynomial in AM_a to adjusted I_{SC} measurements:

$$\frac{I_{SC}}{I_{SC0}\left(1+\alpha_{SC}\left(T_C - T_0\right)\right)}\frac{E_0}{E} = \beta_0 + \beta_1 AM_a + \ldots + \beta_k AM_a^k \quad (5)$$

where typically $k = 4$.

When a two-axis tracker is available, E_b can be directly measured using suitable instruments. The instrument is held normal to the sun thus avoiding reflections from the module's face, and clear-sky periods can be identified from measured E_b. In contrast, when only fixed racking is used, a method is needed to identify clear sky conditions and to estimate E_b and E_{diff} from G_{POA}. While clear sky conditions could be isolated by visual inspection, we automate the process by comparing

G_{POA} to a clear sky model. The Haurwitz clear sky model [12] is used to estimate clear sky GHI, and the DIRINT modification of the DISC model [13] is used to estimate clear sky DNI. Direct irradiance on the plane of array is calculated in the usual manner. The Sandia simple sky diffuse model [14], together with the ground diffuse model in [15], is used to estimate diffuse irradiance on the plane of array. The selected models are able to predict clear-sky irradiance quantities with reasonable accuracy [16]. These quantities are combined to obtain a modeled value for G_{POA} under clear sky conditions.

The G_{POA} measurements are then compared to the modeled clear sky values to identify days with clear sky conditions. For a particular day to be classified as having clear sky conditions, 90% of the data points must meet the following criteria: 1) measured G_{POA} must be within 150 W/m^2 of the corresponding clear sky modeled values and 2) the time derivative of the measured G_{POA} must not exceed 2.5 times the time derivative of clear sky modeled values. Since mPERT includes precipitation data, days with any recorded precipitation were also removed. Fig. 2 illustrates the measured G_{POA} and the subset of the data that is identified with clear sky conditions at Cocoa over the sampling period. The selection criteria for clear sky conditions results in 28 clear sky days at Cocoa, 54 clear sky days at Eugene, and 26 clear sky days at Golden. Clear sky days are distributed throughout the year.

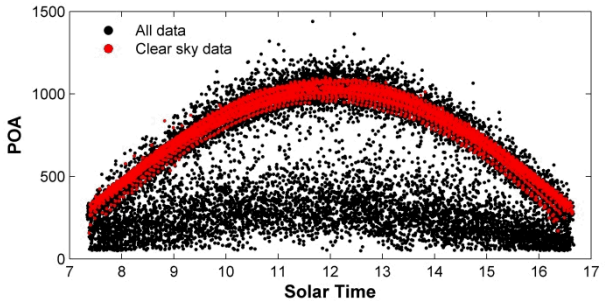

Fig. 2. Measured G_{POA} and subset of measurements estimated to occur during clear-sky conditions during the sampling period at Cocoa.

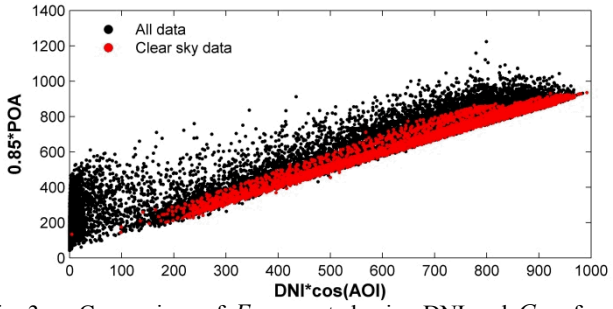

Fig. 3. Comparison of E_b computed using DNI and G_{POA} for clear sky conditions during the sampling period at Cocoa.

For clear sky conditions, E_b and E_{diff} in Eq. 1 are estimated as 85% and 15% of G_{POA}, respectively. Many clear sky models (e.g., [17]) assume similar proportions for beam and sky diffuse irradiance under clear sky conditions. The contribution to E_{diff} from ground reflections can be assumed to be negligible. For comparison, DNI, corrected for AOI, is compared to E_b estimated from G_{POA} for clear sky conditions using data at Cocoa (Fig. 3). After estimating E_b and E_{diff}, Eq. 2 through Eq. 5 are used to estimate I_{SC0} and $f_1(AM_a)$ for each module. The remaining parameters in the SAPM can be calibrated using methods described in [7], [10].

IV. Results

In this paper, $f_1(AM_a)$ and I_{SC0} are estimated for ten modules covering a wide range of cell technologies. The modules include: one single crystalline silicon module (Single c-Si), three multi crystalline silicon modules (Multi c-Si 1,2,3), one cadmium telluride module (CdTe), two copper indium gallium selenide modules (CIGS 1,2), and three amorphous silicon modules (a-Si 1,2,3). The mPERT database contains one additional amorphous silicon module, however, temperature coefficients were not available. Based on site location, sampling time, and module orientation, the range of AM_a in the data varies based on the time of year. For example, very few data points with high AM_a are available in the summer, especially at northern latitudes and high elevations. Given a five or fifteen minute sampling time, it can be difficult to capture data at high AM_a values.

For each module, I_{SC0} was estimated using Eq. 4 and data during days with clear sky conditions over the entire year. An example regression model, fit to the Single c-Si module at Cocoa is shown in Fig. 4. The value of I_{SC0} is defined at AM_a = 1.5. Table I includes estimated I_{SC0} values along with datasheet values for each module. Estimated I_{SC0} values are generally lower than the data sheet value by 3%, on average. Estimated I_{SC0} at Cocoa are systematically higher than the other two locations. Values of I_{SC0} fluctuate very little (< 0.05 A) when estimated at different times of the year.

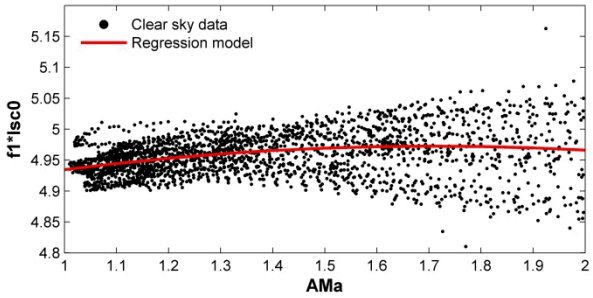

Fig. 4. Regression model used to estimate I_{SC0} for the Single c-Si module at Cocoa.

Table I. Estimated I_{SC0}, datasheet value in parentheses.

	Cocoa	Eugene	Golden
Single c-Si	4.97 (5.13)	4.87 (5.13)	4.89 (5.08)
Multi c-Si 1	4.92 (5.01)	4.80 (5.01)	4.85 (5.00)
Multi c-Si 2	2.66 (2.73)	2.62 (2.73)	2.64 (2.70)
Multi c-Si 3	2.67 (2.73)	2.60 (2.73)	2.64 (2.69)
CdTe	1.16 (1.17)	1.13 (1.17)	1.12 (1.18)
CIGS 1	6.27 (6.32)	6.03 (6.32)	5.90 (5.83)
CIGS 2	2.46 (2.49)	2.41 (2.49)	2.42 (2.52)
a-Si 1	5.35 (5.46)	5.21 (5.46)	5.34 (5.49)
a-Si 2	1.09 (1.12)	1.04 (1.12)	1.10 (1.20)
a-Si 3	4.61 (4.62)	4.51 (4.62)	4.36 (4.62)

After estimating I_{SC0}, $f_1(AM_a)$ can be estimated using Eq. 5. Results show that the air mass modifier has strong seasonal fluctuation at all three sites and for all ten cell technologies. The air mass modifier data, f_1, and best fit $f_1(AM_a)$ polynomial for the Single c-Si and CdTe modules are shown in Fig. 5 and 6, respectively. To illustrate the seasonal dependence, each data point is colored by the day of year. Variability in the air mass modifier for these two modules is characteristic of the other modules. In general, results show higher values in the winter than in the summer. Given the fixed tilt orientation of the panels, AM_a values over 3 are not expected in the summer. The air mass modifiers for the all three Multi c-Si modules, both CIGS modules, and one a-Si module (HIT) have characteristics similar to the Single c-Si module shown in Fig. 5. The remaining two a-Si modules have similar air mass modifier characteristics to the CdTe results shown in Fig 6.

Within a single clear sky day, we note that the f_1 value can differ by up to 5% at the same AM_a between morning and evening. Moreover, for a given module type and location the differences appear to be systematic, e.g., with higher values always occurring in the afternoon. This effect has also been noted in [6].

Significant fluctuation in the fitted polynomials are observed at high air mass (e.g., Eugene data in Fig 6) and sometimes also at low air mass (e.g., Eugene data in Fig. 5). These fluctuations are a consequence of using a polynomial to

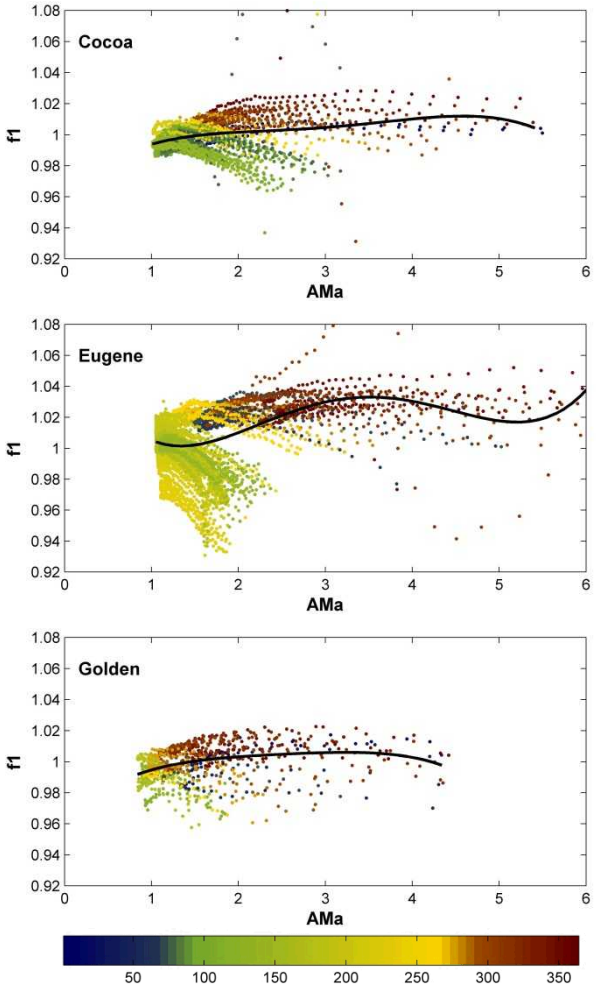

Fig. 5. Air mass modifier for the single c-Si module, data (colored by day of year) along with the $f_1(AM_a)$ polynomial.

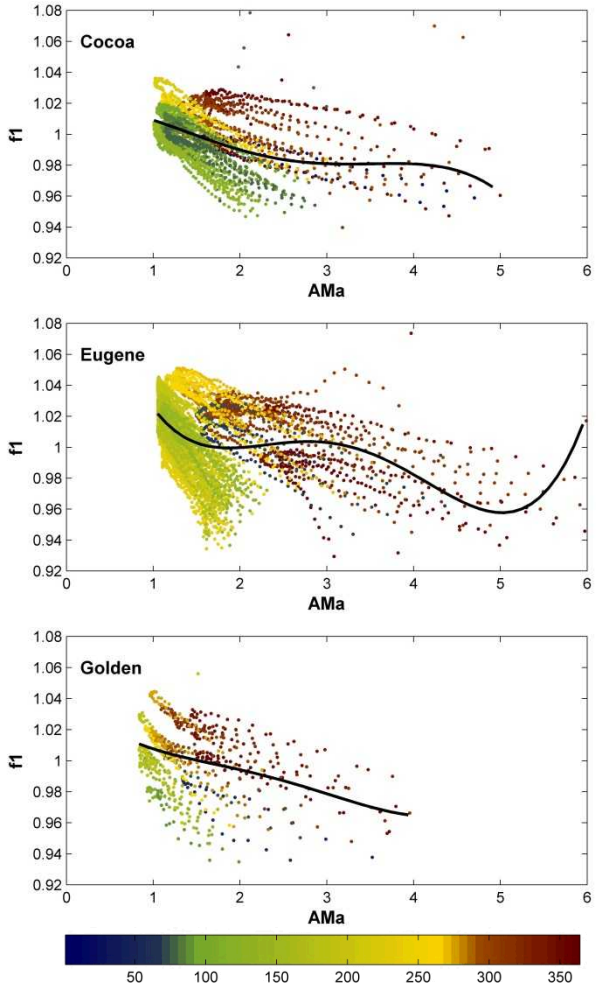

Fig. 6. Air mass modifier for the CdTe module, data (colored by day of year) along with the $f_1(AM_a)$ polynomial.

express f_1. Fitted polynomials are inherently sensitive to small variations in data at the extremes of the fitted data [18]. While fluctuations in f_1 at high air mass may not affect PV model results to any significant degree, fluctuations at low air mass are almost certain to degrade prediction accuracy.

It is our opinion that an alternate expression for f_1 is needed. One potential avenue to improve model accuracy is to reformulate the air mass modifier to account for time of year and time of day as additional predictors. The data in Fig 6 and 7 show generally consistent patterns indicating that a general model for f_1 may be successful across many module technologies, but this model should not be formulated as a polynomial with respect to air mass alone.

V. Conclusions

The use of mPERT data allows for detailed investigation on the impact of spectral variability on short circuit current. In this paper, we demonstrate methods to isolate the air mass modifier and short circuit current at STC using data collected at fixed tilt orientation and track the dependence of location and time of year on these parameters. We find that I_{SC0} is systematically higher at Cocoa than at the other two locations. Estimated I_{SC0} values change very little throughout the year. The air mass modifiers, on the other hand, are highly variable throughout the year at each of the three locations. In general, we find that the air mass modifiers are higher in the winter than in the summer. These effects might be related to the higher absolute humidity in the summer, and overall higher absolute humidity at Cocoa. Additional research is needed.

The use of a single polynomial model in AM_a to model the effect on module current of spectral variation introduces uncertainty into module performance predictions. The single polynomial does not represent systematic locational, seasonal or time of day variation in measured module output. As a result, we view the current polynomial model form as not suitable. These results indicate opportunities to improve prediction accuracy by improvements to the air mass modifier component of performance models.

Acknowledgement

Sandia National Laboratories is a multi-program laboratory managed and operated by Sandia Corporation, a wholly owned subsidiary of Lockheed Martin Corporation, for the U.S. Department of Energy's National Nuclear Security Administration under contract DE-AC04 94AL85000.

References

[1] D. L. King, E. E. Boyson, and J. A. Kratochvil, "Photovoltaic Array Performance Model," Sandia National Laboratories, Albuquerque, NM SAND2004-3535, 2004.

[2] W. De Soto, S. A. Klein, and W. A. Beckman, "Improvement and validation of a model for photovoltaic array performance," *Solar Energy,* vol. 80, pp. 78-88, 2006.

[3] D. L. King, J. A. Kratochvil, and W. E. Boyson, "Measuring solar spectral and angle-of-incidence effects on photovoltaic modules and solar irradiance sensors," in *Photovoltaic Specialists Conference, 1997., Conference Record of the Twenty-Sixth IEEE*, 1997, pp. 1113-1116.

[4] C. Hansen, J. Stein, S. Miller, E. E. Boyson, J. A. Kratochvill, and D. L. King, "Parameter Uncertainty in the Sandia Array Performance Model for Flat-Plate Crystalline Silicon Modules," in *37th IEEE Photovoltaics Specialists Conference*, Seattle, WA, 2011.

[5] J. E. Granata, W. E. Boyson, J. A. Kratochvil, B. Li, V. Abbaraju, G. TamizhMani, and L. Pratt, "Successful Transfer of Sandia National Laboratories' Outdoor Test technology to TUV Rheinland Photovoltaic Testing laboratory," in *IEEE Photovoltaic Specialists Conference*, Seattle, WA, 2011.

[6] C. R. Osterwald, K. A. Emery, and M. Muller, "Photovoltaic module calibration value versus optical air mass: the air mass function," *Progress in Photovoltaics: Research and Applications,* vol. 22, pp. 560-573, 2014.

[7] K. A. Klise, C. W. Hansen, J. S. Stein, Y. Ueda, and K. Hakuta, "Calibration of Photovoltaic Module Performance Models Using Monitored System Data," presented at the 29th European PV Solar Energy Conference, Amsterdam, The Netherlands, 2014.

[8] R. W. Andrews, A. Pollard, and J. M. Pearce, "Improved parametric empirical determination of module short circuit current for modelling and optimization of solar photovoltaic systems," *Solar Energy,* vol. 86, pp. 2240-2254, 2012.

[9] W. Marion, A. Anderberg, C. Deline, S. Glick, M. Muller, G. Perrin, J. Rodriguez, S. Rummel, K. Terwilliger, and T. J. Silverman, "User's Manual for Data for Validating Models for PV Module Performance," National Renewable Energy Laboratory NREL/TP-5200-61610, 2014.

[10] C. W. Hansen, K. A. Klise, J. Stein, Y. Ueda, and K. Hakuta, "Photovoltaic System Model Calibration Using Monitored System Data," presented at the 6th World Conference on Photovoltaic Energy Conversion, Kyoto, Japan, 2014.

[11] A. L. Buck, "New Equations for Computing Vapor Pressure and Enhancement Factor," *Journal of Applied Meteorology,* vol. 20, pp. 1527-1532, 1981/12/01 1981.

[12] B. Haurwitz, "Insolation in Relation to Cloudiness and Cloud Density," *Journal of Meteorology,* vol. 2, pp. 154-166, 1945/09/01 1945.

[13] R. Perez, P. Ineichen, E. L. Maxwell, R. Seals, and A. Zelenka, "Dynamic Global-to-Direct Irradiance Conversion Models," *ASHRAE Transactions,* vol. 98, 1992.

[14] *PV_LIB*. Available: http://pvpmc.org/pv-lib/

[15] P. G. Loutzenhiser, H. Manz, C. Felsmann, P. A. Strachan, T. Frank, and G. M. Maxwell, "Empirical validation of models to compute solar irradiance on inclined surfaces for building energy simulation," *Solar Energy,* vol. 81, pp. 254-267, 2007.

[16] M. J. Reno, C. W. Hansen, and J. S. Stein, "Global Horizontal Irradiance Clear Sky Models: Implementation and Analysis," Sandia National Laboratories, Albuquerque, NM SAND2012-2389, 2012.

[17] D. G. Erbs, S. A. Klein, and J. A. Duffie, "Estimation of the diffuse radiation fraction for hourly, daily and monthly-average global radiation," *Solar Energy,* vol. 28, pp. 293-302, 1982.

[18] L. Magee, "Nonlocal Behavior in Polynomial Regressions," *The American Statistician,* vol. 52, pp. 20-22, 1998.